

1  
2  
3  
4  
5  
6  
7  
8  
9  
10  
11  
12  
13  
14  
15  
16  
17  
18  
19  
20  
21  
22  
23  
24  
25  
26  
27

## The first-in-class peptide binder to the SARS-CoV-2 spike protein

**Authors:** G. Zhang<sup>1</sup>, S. Pomplun<sup>1</sup>, A. R. Loftis<sup>1</sup>, A. Loas<sup>1</sup>, and B. L. Pentelute<sup>1,2\*</sup>

### **Affiliations:**

<sup>1</sup> Massachusetts Institute of Technology, Department of Chemistry, 77 Massachusetts Avenue, Cambridge, MA 02139, USA.

<sup>2</sup> Extramural Member, Koch Institute of Integrative Cancer Research MIT; Associate Member, Broad Institute of Harvard and MIT; Member, Center for Environmental Health Sciences MIT; Cambridge, MA 02139, USA.

\*Correspondence to: [blp@mit.edu](mailto:blp@mit.edu)

28 **Abstract**

29           Coronavirus disease 19 (COVID-19) is an emerging global health crisis. With over 200,000  
30 confirmed cases to date, this pandemic continues to expand, spurring research to discover  
31 vaccines and therapies. SARS-CoV-2 is the novel coronavirus responsible for this disease. It  
32 initiates entry into human cells by binding to angiotensin-converting enzyme 2 (ACE2) via the  
33 receptor binding domain (RBD) of its spike protein (S). Disrupting the SARS-CoV-2-RBD binding  
34 to ACE2 with designer drugs has the potential to inhibit the virus from entering human cells,  
35 presenting a new modality for therapeutic intervention. Peptide-based binders are an attractive  
36 solution to inhibit the RBD-ACE2 interaction by adequately covering the extended protein contact  
37 interface. Using molecular dynamics simulations based on the recently solved ACE2 and SARS-  
38 CoV-2-RBD co-crystal structure, we observed that the ACE2 peptidase domain (PD)  $\alpha$ 1 helix is  
39 important for binding SARS-CoV-2-RBD. Using automated fast-flow peptide synthesis, we  
40 chemically synthesized a 23-mer peptide fragment of the ACE2 PD  $\alpha$ 1 helix composed entirely of  
41 proteinogenic amino acids. Chemical synthesis of this human derived sequence was complete in  
42 1.5 hours and after work up and isolation >20 milligrams of pure material was obtained. Bio-layer  
43 interferometry revealed that this peptide specifically associates with the SARS-CoV-2-RBD with  
44 low nanomolar affinity. This peptide binder to SARS-CoV-2-RBD provides new avenues for  
45 COVID-19 treatment and diagnostic modalities by blocking the SARS-CoV-2 spike protein  
46 interaction with ACE2 and thus precluding virus entry into human cells.

47

48 **Key words**: SARS-CoV-2, peptide binder, protein-protein interaction inhibitor, coronavirus,  
49 COVID-19, rapid response, peptide therapeutic, MD simulation, automated flow peptide synthesis

50

51

## 52 **1. Introduction**

53 A novel coronavirus (SARS-CoV-2) from Wuhan, China, has caused 207,855 confirmed  
54 cases and 8,648 deaths globally, according to the COVID-19 situation report from WHO on Mar  
55 19, 2020 (<https://www.who.int/emergencies/diseases/novel-coronavirus-2019/situation-reports/>),  
56 and the number is continually growing. Similar to the SARS-CoV outbreak in 2002, SARS-CoV-2  
57 causes severe respiratory problems. Coughing, fever, difficulties in breathing and/or shortage of  
58 breath are the common symptoms. Aged patients with pre-existing medical conditions are at most  
59 risk with a mortality rate ~1.5% or even higher in some regions. Moreover, human-to-human  
60 transmission can occur rapidly by close contact. To slow this pandemic and treat infected patients,  
61 rapid development of specific antiviral drugs is of the highest urgency.

62 The closely-related SARS-CoV coronavirus invades host cells by binding the angiotensin-  
63 converting enzyme 2 (ACE2) receptor on human cell surface through its viral spike protein (S) [1-  
64 4]. It was recently established that SARS-CoV-2 uses the same receptor for host cell entry [5, 6].  
65 Recent crystallographic studies of the SARS-CoV-2-S receptor binding domain (RBD) and full-  
66 length human ACE2 receptor revealed key amino acid residues at the contact interface between  
67 the two proteins and provide valuable structural information that can be leveraged for the  
68 development of disruptors specific for the SARS-CoV-2/ACE2 protein-protein interaction (PPI) [7,  
69 8]. Small-molecule inhibitors are often less effective at disrupting extended protein binding  
70 interfaces [9]. Peptides, on the other hand, offer a synthetically accessible solution to disrupt PPIs  
71 by binding at interface regions containing multiple contact “hot spots” [10].

72 We hypothesize that disruption of the viral SARS-CoV-2-RBD-host ACE2 interaction with  
73 peptide-based binders will prevent virus entry into human cells, offering a novel opportunity for  
74 therapeutic intervention. Toward this aim, we launched a campaign to rapidly discover peptide  
75 binders to SARS-CoV-2-RBD. Analyzing the RBD-ACE2 co-crystal structure, we found that  
76 SARS-CoV-2-RBD/ACE2 interface spans a large elongated surface area, as is common for PPIs.

77 We leveraged molecular dynamic simulations and automated fast-flow peptide synthesis [11] to  
78 prepare a 23-mer peptide binder (SBP1) to SARS-CoV-2-RBD, the sequence of which was  
79 derived from the ACE2  $\alpha$ 1 helix. Using bio-layer interferometry, we determined that SBP1 binds  
80 SARS-CoV-2-RBD with low nanomolar affinity (dissociation constant,  $K_D = 47$  nM). SBP1 is a  
81 first-in-class peptide binder to SARS-CoV-2-RBD, potentially inhibiting entry of the virus into  
82 human cells. In addition, the human protein-derived sequence of SBP1 is fully proteinogenic, and  
83 is not expected to be immunogenic. Taken together, computational simulations coupled with  
84 automated flow peptide synthesis technology enable an accelerated discovery loop from design  
85 to experimental validation, and rapidly delivered SBP1 as a promising pre-clinical drug lead.  
86 Antiviral activity studies in mammalian cell cultures are in progress in order to evaluate efficacy  
87 of the current and future optimized peptide binders.

88

## 89 **2. Results**

90

### 91 **Molecular dynamic simulations guide peptide binder design**

92 Using the Amber force field [12], a helical peptide sequence (spike-binding peptide 1,  
93 SBP1) derived from the  $\alpha$ 1 helix of ACE2 peptidase domain (ACE2-PD) in complex with SARS-  
94 CoV-2-RBD was simulated under TIP3P explicit water conditions. Analyzing the simulation  
95 trajectory after 200 ns, we found that SBP1 remains on the spike RBD protein surface in a stable  
96 conformation (Fig. 2B) with overall residue fluctuations smaller than 0.8 nm compared with their  
97 starting coordinates (Fig. 2A). Per-residue analysis along the 200 ns trajectory showed that the  
98 middle residues of SBP1, a sequence we termed SBP2, have significantly reduced fluctuations  
99 (Fig. 2C, 2D), indicating key interactions. The results of this MD simulation suggest that SBP1  
100 and SBP2 peptides derived from the ACE-PD  $\alpha$ 1 helix may alone potentially bind the SARS-CoV-  
101 2 spike RBD protein with sufficient affinity to disrupt the associated PPI.

## 102 **Automated fast-flow peptide synthesis yielded >95% pure compound**

103 The two biotinylated peptides, SBP1 and SBP2, derived from the  $\alpha$ 1 helix were prepared  
104 by automated fast-flow peptide synthesis [11, 13] with a total synthesis time of 1.5 h for a total of  
105 35 couplings. After cleavage from resin, global deprotection, and subsequent C18 solid-phase  
106 extraction, the purity of the crude peptides was estimated to be >95% for both biotinylated SBP1  
107 and SBP2 based on LC-MS TIC chromatograms (supplemental Fig. 1A and 1B). We assessed  
108 this purity as acceptable for direct downstream biological characterizations.

## 109 **SBP1 peptide specifically binds SARS-CoV-2-RBD with low nanomolar affinity**

110 Bio-layer interferometry was employed to measure the affinity of synthesized peptides  
111 (e.g., SBP1) to glycosylated SARS-CoV-2-RBD or the human protein menin as a negative control.  
112 Biotinylated peptide was immobilized onto streptavidin (SA) biosensors. After fitting the  
113 association and dissociation curves from serial dilutions of protein, the dissociation constant ( $K_D$ )  
114 of SBP1 to the RBD was determined to be 47 nM with the average  $K_{on} = 4.69 \times 10^4 \text{ M}^{-1} \text{ s}^{-1}$  and  
115  $K_{off} = 2.2 \times 10^{-3} \text{ s}^{-1}$  (Fig. 2E). However, SBP2 (a truncate of SBP1) did not associate with the spike  
116 RBD protein (Fig. 2F). SBP1 had no observable binding to the negative control human protein  
117 menin (Fig. 2G). Together, these data indicate that SBP1 specifically binds SARS-CoV-2-RBD  
118 with low nanomolar affinity.

119

## 120 **3. Discussion**

121 Recently published cryo-EM and co-crystal structures of the RBD of SARS-CoV-2 with  
122 human ACE2 have identified this PPI as key step for the entry of SARS-CoV-2 to human cells.  
123 Blocking this binding interface represents a highly promising therapeutic strategy, as it could  
124 potentially hinder SARS-CoV-2 from entering cells and replicating.

125           Drugging PPIs is a longstanding challenge in traditional drug discovery and peptide-based  
126 approaches might help to solve this problem. Small molecule compounds are unlikely to bind  
127 large protein surfaces that do not have distinct binding pockets. Peptides, on the other hand,  
128 display a larger surface area and chemical functionalities that can mimic and disrupt the native  
129 PPI, as is the case for the clinically approved HIV peptide drug Fuzeon [14, 15].

130           The identification of a suitable starting point for drug discovery campaigns can be time-  
131 intensive. During a pandemic such as this one, therapeutic interventions are urgently needed. To  
132 rapidly identify potential peptide binders to the SARS-CoV-2 spike protein, we used molecular  
133 dynamics (MD) simulation on peptides extracted from the human ACE2 sequence. The starting  
134 point of the binding simulations was the cryo-electron microscopy model of SARS-CoV-2 spike  
135 protein and several peptides derived from the SARS-CoV-2-spike binding domain of human ACE2  
136 protein. Our MD simulation (200 ns trajectory) indicated that the SBP1 peptide, corresponding to  
137 the *N*-terminal ACE2  $\alpha$ 1 helix, stably bound to SARS-CoV-2-RBD. The overall peptide fluctuations  
138 were smaller than 0.8 nm from starting coordinates (Fig. 2A). These results indicated the potential  
139 of identifying a SARS-CoV-2-RBD-binding peptide derived from the human ACE2  $\alpha$ 1 helix.

140           A 23-mer peptide sequence (SBP1) was synthesized by automated flow peptide synthesis.  
141 The 23 residues selected from the ACE2  $\alpha$ 1 helix sequence (IEEQAKTFLDKFNHEAEDLFYQS)  
142 showed low fluctuations along the MD simulation trajectory and several important interactions  
143 with the spike protein were observed consistently with multiple lines of published data [8, 16]. We  
144 decided to use this peptide (SBP1) as an experimental starting point for the development of a  
145 SARS-CoV-2 spike protein binder. Our rapid automated flow peptide synthesizer [11, 13] enabled  
146 the synthesis of tens of milligrams of SBP1 peptide within minutes. The crude purity was  
147 determined to be >95% and therefore sufficient for binding validation by bio-layer interferometry  
148 (BLI).

149 The interaction between SBP1 and the RBD of SARS-CoV-2 spike protein was validated  
150 by bio-layer interferometry. The  $K_D$ , derived from protein association and dissociation kinetics,  
151 was found to be 47 nM after averaging the fitting values at different protein concentrations (Fig.  
152 2E). This binding affinity is comparable with that of full length ACE2 binding to SARS-CoV-2-RBD  
153 (14.7 nM) [7]. Excess of SBP1 therefore, could potentially cover spike proteins on SARS-CoV-2  
154 surface and outcompete the binding for ACE2. Further optimization of the sequence length and  
155 amino acid composition are in progress, in order produce binders with higher PPI inhibitory activity.

156 SBP1 is a “fully human,” endogenous peptide and therefore likely to be well tolerated by  
157 the human immune system. The amino acid sequence of SBP1 is entirely derived from human  
158 ACE2 and should be recognized as endogenous by the human immune system. This feature  
159 could be highly beneficial in later stages of pre-clinical development. Challenges associated with  
160 peptide drugs, such as proteolytic degradation and rapid renal elimination, will be addressed in  
161 the near future by chemical modifications of the sequence.

162 In conclusion, a peptide sequence derived from human ACE2 was found to bind the  
163 SARS-CoV-2 spike protein RBD with low nanomolar affinity. We believe disruption of the SARS-  
164 CoV-2-RBD/ACE2 binding interface with high-affinity peptides represents a promising strategy for  
165 preventing virus entry in human cells and paves the way for new COVID-19 treatment and  
166 diagnostic modalities. Upon request, we will make available our peptide binder and all upcoming  
167 optimized variants to research facilities testing and developing potential COVID-19 treatments.  
168 Rapid discovery, synthesis, and testing of potential drug leads should help the global scientific  
169 and healthcare communities efficiently address the ongoing crisis.

170

171

172

## 173 **4. Experimental Materials and Methods**

### 174 **GPU-accelerated molecular dynamic simulation**

175 The co-crystal structure of SARS-CoV-2-RBD with ACE2-B<sup>0</sup>AT1 (PDB: 6M17) was chosen as the  
176 initial structure, which was explicitly solvated in an 87 Å<sup>3</sup> box, to perform a 200 ns molecular  
177 dynamical (MD) simulation using NAMD on MIT's supercomputing clusters (GPU node). Amber  
178 force field was used to model the protein and peptide. The MD simulation system was equilibrated  
179 at 300 K for 2 ns. Periodic boundary conditions were used and long-range electrostatic  
180 interactions were calculated with particle mesh Ewald method, with non-bonded cutoff set to 12.0  
181 Å. SHAKE algorithm was used to constrain bonds involving hydrogen atoms. Time step is 2 fs  
182 and the trajectories were recorded every 10 ps. After simulation production runs, trajectory files  
183 were loaded into the VMD software for further analysis.

### 184 **Automated fast-flow peptide synthesis**

185 SBP1 and SBP2 sequences were synthesized at 90 °C on Rink Amide-ChemMatrix resin with  
186 HATU activation using a fully automatic flow-based peptide synthesizer. Amide bond formation  
187 was performed in 8 seconds, and Fmoc groups were removed in 8 seconds with 40% (v/v)  
188 piperidine in DMF. Overall cycle times were about 120 seconds. After completion of fast-flow  
189 synthesis, the resins were washed with DMF (3 x) and then incubated with HATU-activated biotin-  
190 PEG<sub>4</sub>-propionic acid (CAS# 721431-18-1) at room temperature for 1.0 h for biotinylation on the  
191 peptide *N*-terminus.

### 192 **Peptide cleavage and deprotection**

193 After peptide synthesis, the peptidyl resin was rinsed with dichloromethane briefly and then dried  
194 in a vacuum chamber overnight. Next day, approximately 5 mL of cleavage solution (94% TFA,  
195 1% TIPS, 2.5% EDT, 2.5% water) was added into the syringe containing the resin. The syringe  
196 was kept at room temperature for 2 h before injecting the cleavage solution into a 50 mL conical

197 tube. Dry-ice cold diethyl ether (~50 mL) was added to the cleavage mixture and the precipitate  
198 was collected by centrifugation and triturated twice with cold diethyl ether (50 mL). The  
199 supernatant was discarded. Residual ether was allowed to evaporate and the peptide was  
200 dissolved in water with 0.1% TFA for solid-phase extraction.

#### 201 **Solid-phase extraction (SPE)**

202 After peptide cleavage, peptide precipitates were dissolved in water with 0.1% TFA. Agilent Mega  
203 BE C18 column (Part No: 12256130) was conditioned with 5 mL of 100% acetonitrile with 0.1%  
204 TFA, and then equilibrated with 15 mL of water with 0.1% TFA. Peptides were loaded onto the  
205 column for binding, followed by washing with 15 mL of water with 0.1% TFA, and finally, eluted  
206 with 5 mL of 30/70 water/acetonitrile (v/v) with 0.1% TFA.

#### 207 **Liquid chromatography-mass spectrometry (LC-MS)**

208 Peptides were dissolved in water with 0.1% TFA followed by LC-MS analysis on an Agilent 6550  
209 ESI-Q-TOF instrument using an Agilent Jupiter C4 reverse-phase column (2.1 mm × 150 mm, 5  
210 µm particle size). Mobile phases were 0.1% formic acid in water (solvent A) and 0.1% formic acid  
211 in acetonitrile (solvent B). Linear gradients of 1 to 61% solvent B over 15 minutes (flow rate: 0.5  
212 mL/min) were used to acquire LC-MS chromatograms.

#### 213 **Kinetic binding assay using bio-layer interferometry (BLI)**

214 A ForteBio Octet® RED96 Bio-Layer Interferometry system (Octet RED96, ForteBio, CA) was  
215 used to characterize the *in vitro* peptide-protein binding at 30 °C and 1000 rpm. Briefly,  
216 streptavidin (SA) tips were dipped in 200 µL of biotinylated peptide solution (2.5 µM in 1x kinetic  
217 buffer: 1x PBS with 0.1% BSA and 0.05% tween) for the loading step. The tips loaded with peptide  
218 were then sampled with SARS-CoV-2-RBD or menin protein at various concentrations in 1x  
219 kinetic buffer to obtain the association curve. Peptide only was used as reference for background  
220 subtraction. After association, the tips were dipped back into 1x kinetic buffer to obtain the

221 dissociation curve. The association and dissociation curves were fitted with ForteBio Biosystems  
222 using four experimental conditions ( $n = 4$ , global fitting algorithm, binding model 1:1) to obtain the  
223 dissociation constant  $K_D$ .

224

## 225 **Acknowledgements**

226 The authors thank the MIT Supercomputing Center for providing the computational  
227 resources to run MD simulations. This research was supported by MIT start-up and seed funds.  
228 S.P. is supported by a postdoctoral fellowship from Deutsche Forschungsgemeinschaft (award  
229 PO 2413/1-1). MIT has filed a provisional patent application related to this work.

## 230 **Competing interests**

231 B.L.P. is a founder of Resolute Bio and Amide Technologies.

232

233

234 **Figure captions:**

235 **Figure 1. MD-guided target selection for rapid flow synthesis of a SARS-CoV-2-RBD-**  
236 **binding peptide.** Fragments of ACE2-PD domain are docked against SARS-CoV-2 receptor-  
237 binding domain (PDB: 6M17). Low RMSD peptides are rapidly synthesized by fully automated  
238 flow peptide synthesis, and binding to glycosylated SARS-CoV-2-RBD is determined by BLI.

239

240 **Figure 2. Human ACE2-PD domain  $\alpha$ -helix 1-derived SBP1 binds SARS-CoV-2-RBD.** (A)  
241 RMSD for SBP1 docked to SARS-CoV-2-RBD during 200 ns MD simulation. (B) Binding interface  
242 between SARS-CoV-2-RBD and SBP1 after 200 ns simulation. Individual RMSD (C) and average  
243 RMSD (D) values for SBP1 residues over the course of the 200 ns simulation. Arrows indicate  
244 residues contributing key hydrogen bonding interactions (determined using UCSF Chimera,  
245 Version 1.12). Individual residues with RMSD below 5 Å arbitrarily colored green. Binding affinity  
246 of SBP1 and SBP2 to glycosylated SARS-CoV-2-RBD (E, F), and affinity of SBP1 to negative  
247 control human protein menin (G), as determined by bio-layer interferometry.

248

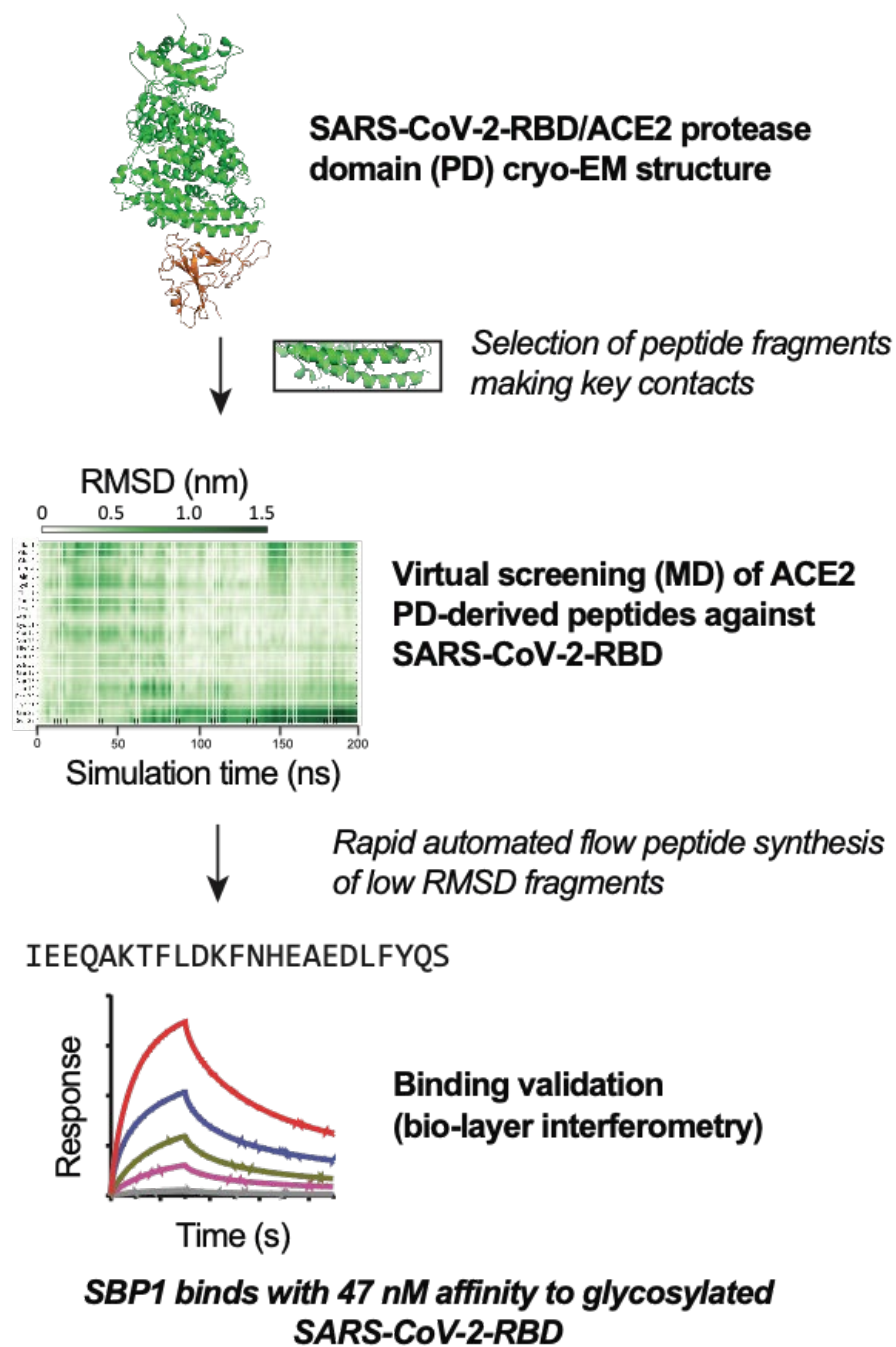
249 **Supplemental Figure 1. ACE2-derived peptides were prepared by solid-phase peptide**  
250 **synthesis.** Total ion current chromatograms (TIC) of purified biotinylated SBP1 peptide (A),  
251 purified biotinylated SBP2 peptide (B), crude SBP1 peptide (C), and crude SBP2 peptide (D).

252

253

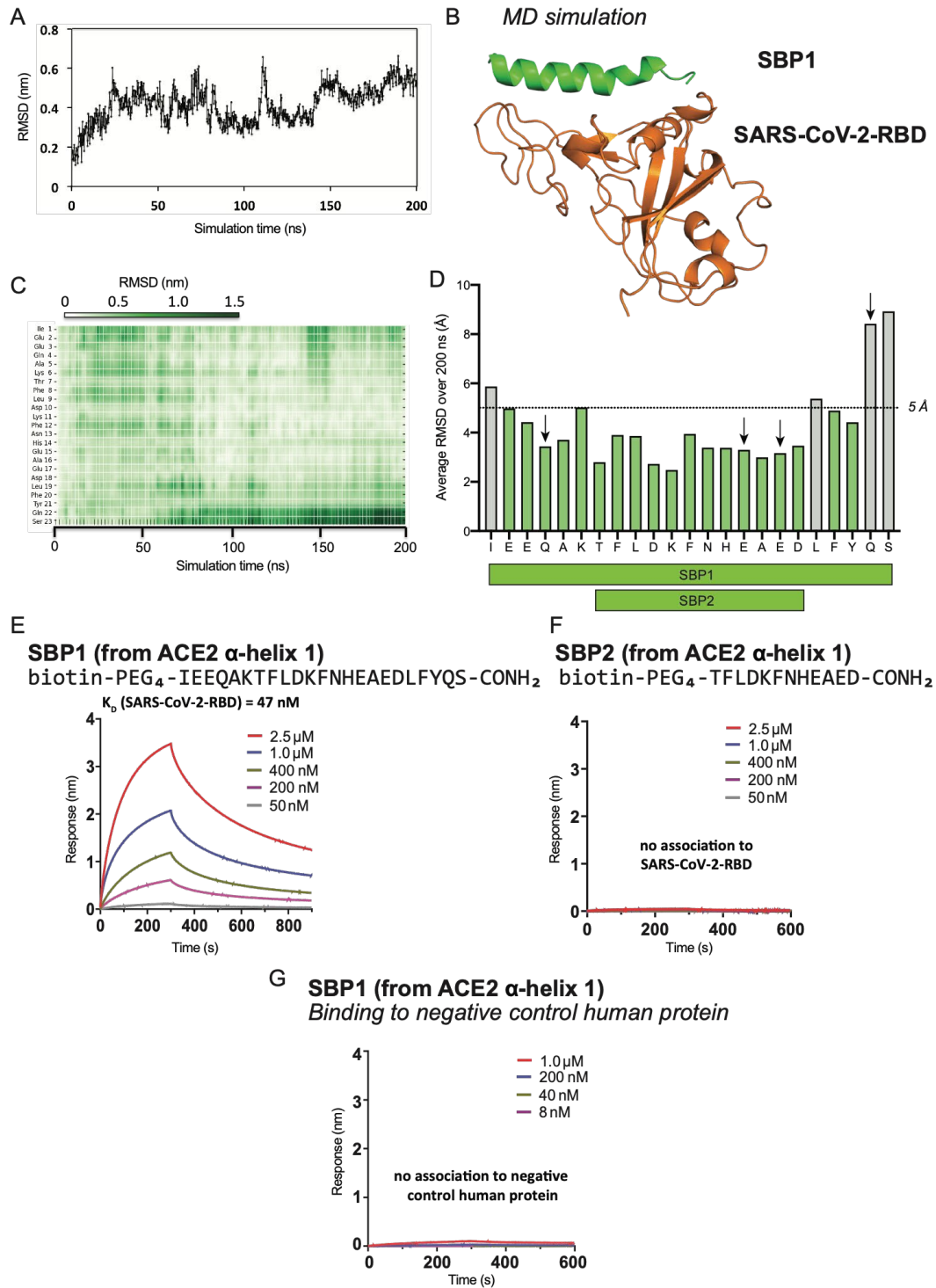
254 **Figures:**

255 **Figure 1**



256

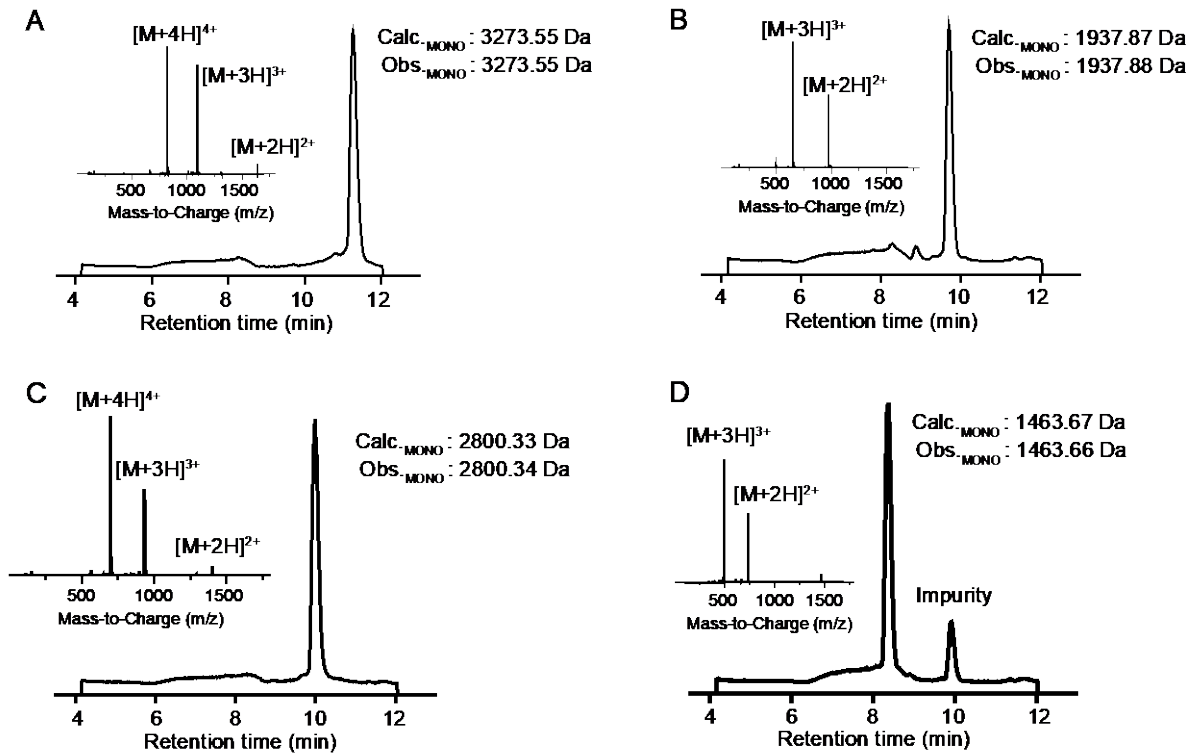
257 **Figure 2**



258

259

260 **Supplemental Figure 1**



261

262

263

## 264 References

- 265 1. F. Li, W. Li, M. Farzan, and S.C. Harrison, *Structure of SARS coronavirus spike receptor-binding*  
266 *domain complexed with receptor*. Science, 2005. **309**(5742): p. 1864-8.
- 267 2. W. Li, C. Zhang, J. Sui, J.H. Kuhn, M.J. Moore, S. Luo, S.K. Wong, I.C. Huang, K. Xu, N. Vasilieva, A.  
268 Murakami, Y. He, W.A. Marasco, Y. Guan, H. Choe, and M. Farzan, *Receptor and viral determinants*  
269 *of SARS-coronavirus adaptation to human ACE2*. EMBO J, 2005. **24**(8): p. 1634-43.
- 270 3. P.B. McCray, Jr., L. Pewe, C. Wohlford-Lenane, M. Hickey, L. Manzel, L. Shi, J. Netland, H.P. Jia, C.  
271 Halabi, C.D. Sigmund, D.K. Meyerholz, P. Kirby, D.C. Look, and S. Perlman, *Lethal infection of K18-*  
272 *hACE2 mice infected with severe acute respiratory syndrome coronavirus*. J Virol, 2007. **81**(2): p.  
273 813-21.
- 274 4. M.J. Moore, T. Dorfman, W. Li, S.K. Wong, Y. Li, J.H. Kuhn, J. Coderre, N. Vasilieva, Z. Han, T.C.  
275 Greenough, M. Farzan, and H. Choe, *Retroviruses pseudotyped with the severe acute respiratory*  
276 *syndrome coronavirus spike protein efficiently infect cells expressing angiotensin-converting*  
277 *enzyme 2*. J Virol, 2004. **78**(19): p. 10628-35.
- 278 5. M. Hoffmann, H. Kleine-Weber, S. Schroeder, N. Kruger, T. Herrler, S. Erichsen, T.S. Schiergens, G.  
279 Herrler, N.H. Wu, A. Nitsche, M.A. Muller, C. Drosten, and S. Pohlmann, *SARS-CoV-2 Cell Entry*  
280 *Depends on ACE2 and TMPRSS2 and Is Blocked by a Clinically Proven Protease Inhibitor*. Cell, 2020.
- 281 6. A.C. Walls, Y.J. Park, M.A. Tortorici, A. Wall, A.T. McGuire, and D. Veesler, *Structure, Function, and*  
282 *Antigenicity of the SARS-CoV-2 Spike Glycoprotein*. Cell, 2020.
- 283 7. D. Wrapp, N. Wang, K.S. Corbett, J.A. Goldsmith, C.L. Hsieh, O. Abiona, B.S. Graham, and J.S.  
284 McLellan, *Cryo-EM structure of the 2019-nCoV spike in the prefusion conformation*. Science, 2020.  
285 **367**(6483): p. 1260-1263.
- 286 8. R. Yan, Y. Zhang, Y. Li, L. Xia, Y. Guo, and Q. Zhou, *Structural basis for the recognition of the SARS-*  
287 *CoV-2 by full-length human ACE2*. Science, 2020.
- 288 9. M.C. Smith, and J.E. Gestwicki, *Features of protein-protein interactions that translate into potent*  
289 *inhibitors: topology, surface area and affinity*. Expert Rev Mol Med, 2012. **14**: p. e16.
- 290 10. K. Josephson, A. Ricardo, and J.W. Szostak, *mRNA display: from basic principles to macrocycle drug*  
291 *discovery*. Drug Discov Today, 2014. **19**(4): p. 388-99.
- 292 11. N. Hartrampf, A. Saebi, M. Poskus, Z.P. Gates, A.J. Callahan, A.E. Cowfer, S. Hanna, S. Antilla, C.K.  
293 Schissel, A.J. Quartararo, X. Ye, A.J. Mijalis, M.D. Simon, A. Loas, S. Liu, C. Jessen, T.E. Nielsen, and  
294 B.L. Pentelute, *Synthesis of proteins by automated flow chemistry*. ChemRxiv, 2020. Preprint:  
295 <https://doi.org/10.26434/chemrxiv.11833503.v1>.
- 296 12. *Amber 2019 reference manual*. <https://ambermd.org/doc12/Amber19.pdf>.
- 297 13. A.J. Mijalis, D.A. Thomas, 3rd, M.D. Simon, A. Adamo, R. Beaumont, K.F. Jensen, and B.L. Pentelute,  
298 *A fully automated flow-based approach for accelerated peptide synthesis*. Nat Chem Biol, 2017.  
299 **13**(5): p. 464-466.
- 300 14. P. Wojcik, and L. Berlicki, *Peptide-based inhibitors of protein-protein interactions*. Bioorg Med  
301 Chem Lett, 2016. **26**(3): p. 707-713.
- 302 15. E.R. Jenny-Avital, *Enfuvirtide, an HIV-1 fusion inhibitor*. N Engl J Med, 2003. **349**(18): p. 1770-1.
- 303 16. Y. Wan, J. Shang, R. Graham, R.S. Baric, and F. Li, *Receptor recognition by novel coronavirus from*  
304 *Wuhan: An analysis based on decade-long structural studies of SARS*. J Virol, 2020.

305